Single-, triple-, or multiple-band Hubbard models

H. Eskes and G. A. Sawatzky
Materials Science Centre, Department of Solid State and Applied Physics, University of Groningen, Nijenborgh 18, 9747 AG Groningen, The Netherlands
(Received 15 March 1991)

The relevance of different models, such as the one-band t-J model and the three-band Emery model, as a realistic description of the electronic structure of high-T_c materials is discussed. Starting from a multiband approach using cluster calculations and an impurity approach, the following questions are addressed: What is the stabilization energy of the Zhang-Rice singlet and triplet with respect to other symmetry levels (such as the $d_{3z^2-r^2}$, etc.)? How does the oxygen $2p$-band width (t_{pp}) influence the stability of the Zhang-Rice singlet? How large is the dispersion of the singlet state? It is argued that, if the one-band model does not give a satisfactory description of the low-energy physics, then the three-band model will be incomplete as well.

I. INTRODUCTION

It is by now widely accepted that the insulating parent compounds of the high-T_c cuprates should be viewed as charge-transfer-gap insulators in which the first ionization state is predominantly of O $2p$ character and the first electron affinity state, predominantly of Cu $3d$ character, with a band gap of about 1.5–2 eV. The strongest and most direct evidence for this comes from photoemission spectroscopy (PES) and resonant photoemission both on the high T_c's (Refs. 1–3) and the related CuO (Refs. 4,5) compound which places the Cu d^8-like electron removal states at much higher energies than the $d^9\underline{L}$-like states. The high-energy electron-energy-loss spectroscopy (ELS)[6] and x-ray absorption (XAS) measurements[7,8] at the O $1s$ threshold of the doped or substituted materials can be considered as a strong confirmation of this conclusion. According to the Zaanen-Sawatzky-Allen (ZSA)[9–11] classification scheme, this situation occurs, provided that the Cu d-d Coulomb interaction (U_d) is larger than the O $2p$–Cu $3d$ charge-transfer energy (Δ).

It is also widely accepted that the low-energy-scale physics of insulating compounds can be well described with a Heisenberg-like Hamiltonian with a superexchange interaction (J) coupling nearest-neighbor spins localized primarily on the Cu ions to form an antiferromagnetic (AF) ground state. The most direct evidence for this comes from neutron diffraction studies[12,13] which are supported by NMR[14,15] and muon[16–18] studies. Remarkable in these studies is the exceptionally large superexchange interaction ($J \sim 0.12$ eV),[19] which is strong evidence for very large Cu-O hybridization effects. Also NMR measurements[20] suggest the spin is not nearly as localized on the Cu as some may want to believe. Small cluster[21–26] as well as impuritylike calculations,[3,27,28] indicate that the spin is located in $d_{x^2-y^2}$ orbitals with about 70% of the spin density on the Cu and 30% distributed over the four neighboring O sites.

That these initial holes are primarily situated in $d_{x^2-y^2}$ symmetry states is confirmed by polarization-dependent ELS and XAS on the Cu $2p$ edge.[6,29] Also the large anisotropic temperature-independent van Vleck susceptibility[30] for magnetic fields perpendicular to the CuO_2 planes is direct evidence for primary x^2-y^2 symmetry for the initial hole since a $d_{3z^2-r^2}$-like state would not contribute to a van Vleck susceptibility for this direction of the field. All of this seems consistent with a three-band Hubbard-like picture involving the Cu $3d_{x^2-y^2}$ states hybridizing with O $2p_x$ and $2p_y$ states pointing towards the copper atoms. Earlier Anderson[31] impurity calculations[27] and cluster calculations,[21,24] however, suggest that other d states like the $d_{3z^2-r^2}$ and perhaps even d_{xy}, d_{xz}, d_{yz} states could be of quite some importance especially in the doped materials since in the ionization spectra these states are energetically close to the lowest energy state. This would suggest that a multiband approach is required.

Most of the theoretical discussions do not start with a multiband problem. Although some stress the importance of the $d_{3z^2-r^2}$ orbitals,[29,32–34] it is commonly believed that the only relevant orbits are the $d_{x^2-y^2}$ and p_σ ones. One of the well-known models is due to Emery.[35] In this model the *AF* compounds consist of holes on Cu, coupled by the superexchange interaction derived from fourth-order perturbation theory in the Cu-O hopping (t_{pd}). Doping will lead to holes on the oxygen, which are coupled to the Cu spins by means of a much larger second-order exchange term and which can move also by means of a second-order hopping process. As pointed out by Varma *et al.*,[36] this so-called three-band model is directly related to the charge-transfer-gap insulators in the ZSA[9] classification scheme. At the other extreme, it has been suggested that a single-band Hubbard approach with a large effective U, which results in a t-J model may be sufficient for these materials.[37]

Zhang and Rice[38] argued that a charge-transfer-gap insulator, which would in principle require at least a two-band approach, could still be described in a single-band

Hubbard framework provided that the Cu-O hopping (t_{pd}) is small with respect to the Coulomb interactions on Cu (U_d) and the charge transfer energy (Δ) and that the O-O hopping integral (t_{pp}) can be neglected. The idea is that the extra hole will form a coherent state on the four oxygens around a Cu atom, and that the two spins will form a singlet. Thus adding holes on oxygen is then equivalent to removing spins from the Cu positions, and these local singlets then dilute and propagate in an antiferromagnetic lattice just as in a single-band Hubbard system.

The O bandwidth or the O-O nearest-neighbor hopping integrals (t_{pp}) are known to be large and should be included in a realistic approach. Using the Anderson impuritylike approach we[27] showed that such a Zhang-Rice singlet was stable even for quite a large O bandwidth. We found that for reasonable parameters singlet bound states are formed. These bound states were, however, found to be energetically close to the top of the O $2p$ band in the impurity limit suggesting that "banding" of these states when including the translational symmetry (Anderson lattice) would cause overlap and mixing with other states. Emery and Reiter[39] (ER) have shown that the real Zhang-Rice singlet will mix strongly with the corresponding triplet at the Brillouin-zone boundary (ER phase conventions). Another state with which the ZR singlet mixes is that involving a $d_{3z^2-r^2}$ orbital, because of the hybridization between the $3z^2-r^2$ and x^2-y^2 Bloch states. This occurs for k vectors away from the Γ point with a maximum mixing at $(\pi,0)$ along the $(0,0)-(\pi,0)$ line. This mixing, if important, would necessitate a multiband Hubbard-like approach.

In this paper we address the question of the applicability of a single-band Hubbard approach. Here we start from a multiband approach, including all five Cu $3d$ and the six O $2p$ orbitals per unit cell of the CuO_2 plane. The electronic structure is treated from a local point of view, using cluster calculations (CuO_4, Cu_2O_{7-8}) and an Anderson impurity approach. The energy positions of the different symmetries (orbitals) are discussed in detail. The effect of the shape of the oxygen band structure on the stability of the Zhang-Rice singlet is discussed using the impurity calculation. We compare singlet-spin trial-wave functions with the low-energy states in the Cu_2O_7 cluster and derive the hopping term (t and t') in the t-t'-J model. The spectral distribution of the singlet-spin and triplet-spin trial-wave functions is compared with the d spectral weight as measured in photoemission.

II. ZHANG-RICE SINGLET VERSUS OTHER SYMMETRY STATES

In order to choose between single and multiband models it is important to know the energy positions of the many possible configurations. The simplest sensible many-band calculation one can do showing these configurations is to consider a CuO_4 cluster. In the calculation we include all 12 oxygen $2p$ orbitals and the 5 copper $3d$ levels. The ground state representing the insulating compounds is now equivalent to introducing one hole in the full shell $d^{10}p^6$ system. The solution is given by a two by two matrix involving the $d_{x^2-y^2}$ orbital and the linear combination of four orbitals on oxygen of the same symmetry ($\underline{L}_{x^2-y^2}$). The photoemission spectrum is calculated by introducing an extra hole in the cluster. A detailed description of the calculation is given in a previous paper.[23] The two-hole calculation involves all the d^8 Coulomb and exchange interactions on the Cu site, given in Table I in terms of the Racah A, B, and C parameters, and also the Coulomb/exchange interactions for two holes on the same oxygen atom (in terms of the Slater F_0 and F_2 integrals).

TABLE I. The various d^8 Coulomb and exchange multiplets expressed in terms of the three Racah parameters A, B, and C. The labels with capitals give the irreducible representation of the two hole singlet (1) and triplet (3) states for the D_{4h} point group. The lower case labels correspond to the d orbitals as follows: $a_1 \rightarrow 3z^2-r^2$, $b_1 \rightarrow x^2-y^2$, $b_2 \rightarrow xy$, $e \rightarrow xy,yz$.

^3E	eb_1	ea_1	eb_2		$^3A_2$	b_1b_2	ee
eb_1	$A-5B$	$-3B\sqrt{3}$	$3B$		b_1b_2	$A+4B$	$6B$
ea_1	$-3B\sqrt{3}$	$A+B$	$-3B\sqrt{3}$		ee	$6B$	$A-5B$
eb_2	$3B$	$-3B\sqrt{3}$	$A-5B$				
^1E	eb_1	ea_1	eb_2		$^1B_1$	a_1b_1	ee
eb_1	$A+B+2C$	$-B\sqrt{3}$	$-3B$		a_1b_1	$A+2C$	$-2B\sqrt{3}$
ea_1	$-B\sqrt{3}$	$A+3B+2C$	$-B\sqrt{3}$		ee	$-2B\sqrt{3}$	$A+B+2C$
eb_2	$-3B$	$B\sqrt{3}$	$A+B+2C$				
$^1A_1$	a_1a_1	b_1b_1	b_2b_2	ee		$^3B_1$	a_1b_1
a_1a_1	$A+4B+3C$	$4B+C$	$4B+C$	$(B+C)\sqrt{2}$		a_1b_1	$A-8B$
b_1b_1	$4B+C$	$A+4B+3C$	C	$(3B+C)\sqrt{2}$			
b_2b_2	$4B+C$	C	$A+4B+3C$	$(3B+C)\sqrt{2}$		$^1A_2$	b_1b_2
ee	$(B+C)\sqrt{2}$	$(3B+C)\sqrt{2}$	$(3B+C)\sqrt{2}$	$A+7B+4C$		b_1b_2	$A+4B$

The parameters used in the calculations are for a large part obtained by comparing the model calculations with photoemission data[23] and are listed in Table II. These values correspond very well with the values obtained from the constrained LDA calculations of Hybertsen *et al.*[40] and McMahan *et al.*,[28,41] which we also included in the table. The parameters t_{pp} and t_{pd} are parameters used in the three-band model.

The issue here is the character of the states which are close to the Fermi level. In Fig. 1 we show the d-spectral weight starting from the one-hole ground state. The low-energy part of the spectrum is of mainly oxygen character ($d^9\underline{L}$) and the states above about 8 eV binding energy correspond mainly to the various d^8 multiplets as given in Table I.

The d-electron removal spectral weight is in fact composed of a number of different local symmetry parts corresponding to the irreducible representations spanned by 2 d holes in a D_{4h} point group. In Fig. 1 we use this D_{4h} point group notation to label the different eigenstates appearing in the calculation. Using Table I one can find the compositions of the wave functions belonging to these labels. The lowest state in Fig. 1 is a singlet A_1 ($^1A_1$) state. This state consists mainly (>99%) of two holes in orbitals of $x^2-y^2(b_1)$ symmetry, with roughly one hole on the copper and one hole on oxygen (68% $d^9\underline{L}$ character). The hole added to reach this state from the ground state has 81% oxygen character and 19% copper character, demonstrating the charge transfer nature of the insulator. Because of this character it can be identified with the Zhang-Rice singlet.

The Zhang-Rice triplet corresponds to the $^3A_1$ state in Fig. 1. As can be seen, this state is about 3.5 eV higher in energy as the singlet, and this large energy difference is in fact the reason why ZR neglect this state. The $^3A_1$ state does not appear in Table I because there is no such state

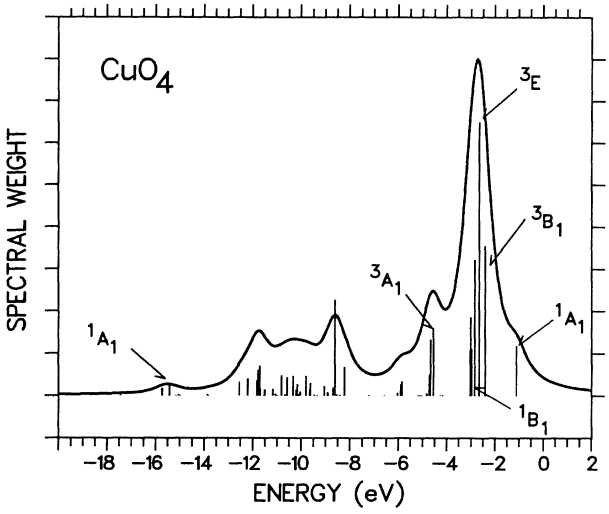

FIG. 1. Cu 3d spectral weight for the CuO_4 cluster calculated for the parameters of Table II. Also shown are some of the symmetry labels (D_{4h} point group) of the two hole singlet and triplet final states.

with two holes on the Cu because of the Pauli exclusion principle. Looking at Fig. 1 one can see that there is really a manifold of states in between the ZR singlet and triplet. The one closest to the ZR singlet ($\simeq 1.5$ eV in energy) is a $^3B_1$ state, involving $3z^2-r^2$ character. This $^3B_1$ state is again of mainly $d^9\underline{L}$ character, but now with one of the holes in a $d_{x^2-y^2}$ orbital and the other in a $d_{3z^2-r^2}$ orbital. It should be noted that the inclusion of the apex oxygen will further stabilize this $^3B_1$ state and in the case

TABLE II. The parameter values used in the calculations, as found by comparing impurity and cluster calculations with spectroscopic experiments. Also shown are estimates from density functional calculations by McMahan *et al.* and Hybersen *et al.* All energies in eV.

Parameter	Experimental	MMS (Ref. 40)	HSC (Ref. 39)
Δ	2.75–3.75 (3.5)	$\Delta_{x^2-y^2}=3.5$	2–4 (3.6)
$(pd\sigma)$	1.5 ($t_{pd}=1.3$)	1.7	1.5
($t_{pd}=1/2\sqrt{3}(pd\sigma)$)			
$(pd\pi)$	−0.7	. . .	. . .
$(pp\sigma)$	−1.0 ($t_{pp}\simeq 0.65$)	$t_{pp}=0.6$	$t_{pp}=0.65$
($t_{pp}=\frac{1}{2}((pp\pi)-(pp\sigma))$)			
$(pp\pi)$	0.3		
U_d	8.8	9.4	9–11 (10.5)
($=A+4B+3C$)	($A=6.5$		
	$B=0.15$		
	$C=0.58$)		
U_p	6	4.7	3–8 (4)
($=F_0+0.16F_2$)	($F_0=5$		
	$F_2=6$)		
U_{pd}	<1(0)	0.8	0.7–1.7 (1.2)

where the apex O–Cu distance is equal to the in-plane Cu-O distance (O_h symmetry), the $^3B_1$ state (Hund's-rule ground state) will be the lowest energy state, as for example is in NiO. This will be discussed further below. The next state is of $^1B_1$ character (a singlet involving $3z^2-r^2$) and after that states of xy, xz, and yz character appear in the main peak of the spectrum. Thus we conclude that the three-band model, including the ZR singlet and triplet, largely overlaps a manifold of states of other symmetries!

Another way to approach the electronic structure of the cuprates is by means of an impurity calculation, based on the following simplifications:

The oxygens on their own are known to form a broad band (~ 5 eV total bandwidth) because of t_{pp}, and also the internal structure of the oxygen bands will be of importance. As the number of holes per oxygen atom is very low, the Coulomb interactions on the oxygen can safely be neglected. Thus the square oxygen lattice is modeled by **k**-dependent tight-binding Bloch states.

On the other hand, one likes to retain the explicit Coulomb and exchange interactions on Cu. This can be done if one neglects the Cu periodicity, i.e., only considers one Cu atom. This approximation is reasonable if the Cu orbitals form narrow bands (which seems to be the case except perhaps for the $d_{x^2-y^2}$ ones).

Thus the model consists of one Cu "impurity" embedded in an oxygen lattice. Again the "half-filled-band" ground state is given by a one-hole calculation. Photoemission is a two-hole problem, which can be solved exactly by means of Green's functions, as described in detail before.[42–44,27] The Hamiltonian reads

$$H = H_0 + H_1 ,$$

$$H_0 = \sum_{\alpha,\sigma} \varepsilon_\alpha d^\dagger_{\alpha,\sigma} d_{\alpha,\sigma} + \sum_{\beta,\mathbf{k},\sigma} \varepsilon_\beta(\mathbf{k}) c^\dagger_{\beta,\mathbf{k},\sigma} c_{\beta,\mathbf{k},\sigma} + \sum_{\alpha,\beta,\mathbf{k},\sigma} [V_{\alpha\beta}(\mathbf{k}) c^\dagger_{\beta,\mathbf{k},\sigma} d_{\alpha,\sigma} + \text{H.c.}] , \quad (1)$$

$$H_1 = \sum_{\alpha,\beta,\gamma,\delta,\sigma,\sigma'} U(\alpha,\beta,\gamma,\delta,\sigma,\sigma') d^\dagger_{\alpha,\sigma} d_{\beta,\sigma} d^\dagger_{\gamma,\sigma'} d_{\delta,\sigma'} .$$

The second term in the Hamiltonian (H_1) describes the interactions on the Cu site, and the values of U can be found in Table I. The first term describes the one-particle part. The operator $d_{\alpha,\sigma}$ annihilates holes on the Cu site with spin σ. The label α enumerates the five d orbitals. The second term in H_0 counts the number of oxygen holes in the Bloch state with momentum **k**, orbital label β (x, y, or z), and spin σ. The last term describes the **k**-dependent coupling of the Bloch state with the Cu site. As an example, we have

$$\varepsilon_x(\mathbf{k}) = 2(pp\sigma)\cos(k_x) + 2(pp\pi)\cos(k_y) ,$$
$$V_{x^2-y^2,x}(\mathbf{k}) = i\sqrt{6}(pd\sigma)\cos(\tfrac{1}{2}k_x)\sin(\tfrac{1}{2}k_y) . \quad (2)$$

The solution of the one-hole Green's function involves an integration over the two-dimensional k space, which is evaluated numerically.

The two-hole Green's functions, or the photoemission spectrum, can be expressed in terms of the one-hole Green's functions and the matrix elements given in Table I. For details the reader is referred to Ref. 27 and Ref. 44.

$$\langle d,\alpha|\hat{G}|d,\alpha\rangle = \left[z - \varepsilon_\alpha - \frac{1}{(2\pi)^2} \int d\mathbf{k} \sum_\beta \frac{V_{\alpha\beta}(\mathbf{k})^2}{z-\varepsilon_\beta(\mathbf{k})} \right]^{-1} \quad (3)$$

In Fig. 2(a) we compare the d-electron removal spectral weight of such an impurity calculation for the parameters of Table I with the XPS spectrum of CuO. Important is that both the energy scale of the observed structure and the relative intensity of the satellite and main line regions are reproduced by the theory for the parameter set of Table I. Furthermore, the spectrum is qualitatively very similar to the one in Fig. 1. Note that most of the discrete levels in Fig. 1 have now become bands. The lowest oxygen band level lies at 2.7 eV in Fig. 2. In Fig. 2(b) we again show the partial d-electron removal spectral weights for each of the irreducible representations of Table II. For these parameters the lowest energy state is

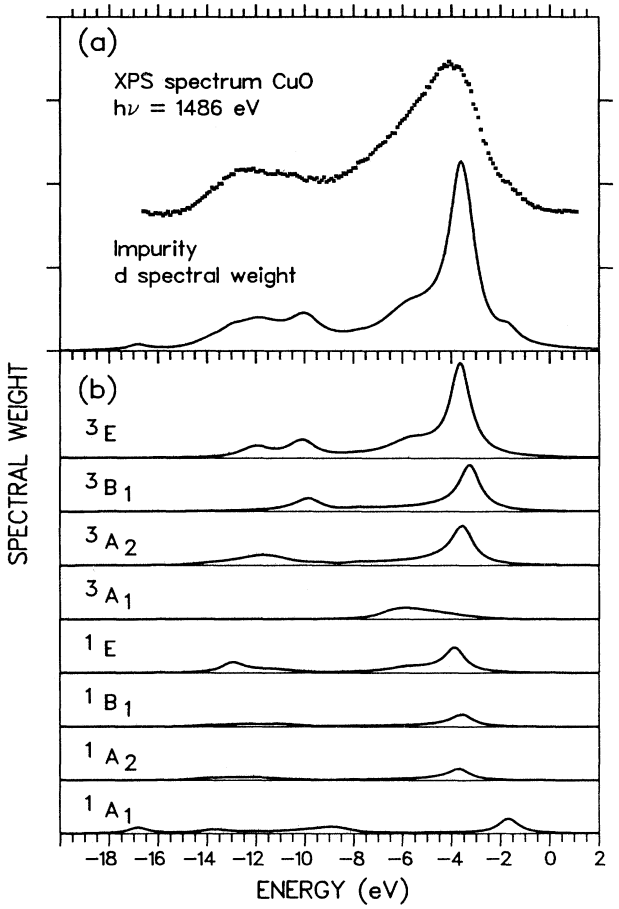

FIG. 2. The d-spectral weight from the impurity calculation using the parameters in Table II. (a) also shows the experimental XPS spectrum for CuO. The contribution of the various symmetry components is shown in (b) (D_{4h} point group).

again of $^1A_1$ symmetry. In the impurity calculation this state is a discrete level pushed out of the top of the oxygen band. The energy separation of this state (ZR singlet) to the lowest oxygen level, however, is not very large (1 eV). It is this splitting as compared with the dispersion of the ZR singlet which gives a measure of the stability of this state.

III. ZHANG-RICE SINGLET VERSUS OXYGEN BANDING

In this section the consequences of the finite oxygen bandwidth are investigated and a quantitative estimate of the stabilization energy of the ZR singlet with respect to the continuum of oxygen states is made. The effect of the character (symmetry) of the oxygen Bloch states on this stabilization energy is discussed.

As already said, in their original paper[38] ZR neglect the oxygen hopping parameter t_{pp}. In this case the zeroth-order (in t_{pd}) ground-state configuration consists of spins on the Cu sites with x-immobile holes per CuO_2 unit on oxygen sites, where x is the amount of hole doping. If one now increases the size of t_{pd}, these holes tend to form singlets with the Cu spins. If one, however, starts with a finite t_{pp} the situation becomes quite different. In this case the zeroth-order state consists of mobile holes described in terms of Bloch states. If one now switches on the Cu-O hopping t_{pd} these mobile holes will scatter off the localized spins formed by the Cu sublattice, and the whole situation looks more like a Kondo problem. In order to choose between these two scenarios one has to go beyond the second-order perturbation theory and to do a calculation with realistic values of t_{pp} and t_{pd}.

The impurity problem as described above in fact includes both limits, that of localized singlet states and itinerant oxygen scattering states. Therefore it is an ideal tool to investigate which of the two pictures is the most reliable one. In Fig. 3 we sketch the various possible situations for an impurity in a metallic or semiconducting host, demonstrating the difference between a Mott-Hubbard (b) and a charge transfer gap (d) insulator, and the relation with the Kondo problem (a). For our purposes here Fig. 3(e) is of the most importance. This situation occurs if the hybridization of the impurity with the O $2p$ band is sufficiently strong to push out a bound state from the top of the O $2p$ band. This bound state (of which there can be one for each possible d^8 multiplet) has the spin and symmetry of Cu d^8 states but the charge is largely on the oxygen. This is similar to the Haldane-Anderson[45] multiply charged impurity states in semiconductors. The single Hubbard band approach will only be valid if, in the impurity limit, a singlet bound state is pushed sufficiently far above the O $2p$ band so that it will retain its identity even if the translation symmetry of the Cu ions is included causing this bound state to form a band. Thus an important parameter in Fig. 3(e) is δ, which is the energy difference between the singlet bound state and the band of itinerant oxygen states.

Let us first model the oxygen band structure by a simple semispherical density of states [as shown in Fig. 4(a)]

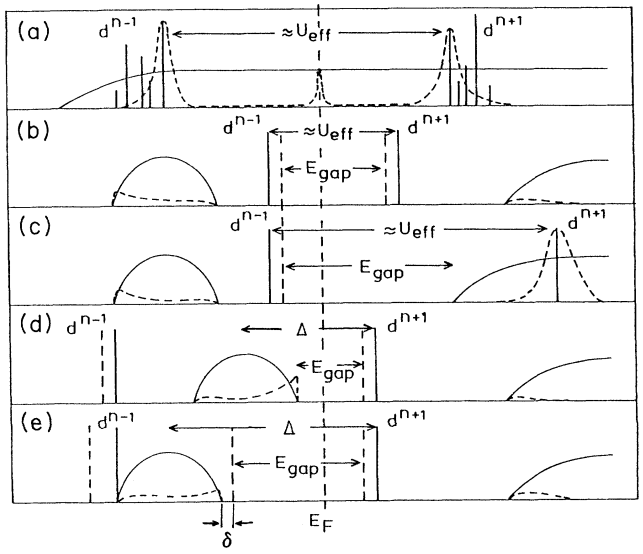

FIG. 3. The various situations one can encounter when introducing d- or f-shell impurities in a metallic or insulating host. (a) sketches the situation for the Kondo problem. The Mott-Hubbard insulating case is shown in (b), and (d),(e) correspond to charge transfer insulators. The important parameters are the charge transfer energy (Δ) and the Coulomb interaction on the impurity (U_{eff}). The dashed lines show the effect of hybridization between the itinerant and localized states.

with a Cu-O hopping $V_{pd}(\varepsilon)$, which is independent of the energy ε. Restricting our discussion to the CuO planes, the oxygens form a simple two-dimensional square lattice and the total bandwidth in terms of the Slater-Koster parameters is $W=4(pp\pi-pp\sigma)$. With the parameters in Table II one finds a total bandwidth of about 5 eV. Using this form for the oxygen band we calculate the curves of constant stabilization energy of the singlet (δ) as a function of the charge transfer energy Δ and the oxygen bandwidth W. The results are shown in Fig. 5. All parameters are scaled with t_{pd}. In this plot we keep the difference between A and Δ constant $[(A-\Delta)/t_{pd}=2.3]$, which is required to obtain the correct energy scale in the XPS spectrum. Also shown in the figure are the contours of constant energy gap (E_{gap}) defined as

$$E_{gap}=E_{min}^{N-1}-E_g^N+E_{min}^{N+1}-E_g^N , \tag{4}$$

where N refers to the total number of electrons. This is just the minimum energy required to remove one electron from the system, plus that to add one electron to the system. From Fig. 5 we see that the increase of the O $2p$ bandwidth causes a destabilization of the Zhang-Rice singlet. This effect is really quite large and may indeed cause a breakdown of the t-J model. For an oxygen bandwidth of about 3 eV and $\Delta/t_{pd}=2.5$ eV the Zhang-Rice singlet is already only 0.5 eV from the top of the O $2p$ band, and taking again the parameters of Table II

one sees that δ is about 0.3 eV, which is of the same order of magnitude as the superexchange interaction J. This is not enough to form a singlet band clearly separated from other degrees of freedom, and a one-band model does not seem to be appropriate.

The internal structure of the oxygen band is, however, very important.[23,46] Using Eqs. (2) the isotropic hybridization [Fig. 4(a)] is replaced by an energy- and orbital-dependent one. In Fig. 4(b) we sketch how the different Cu d orbital symmetries are distributed over the oxygen band (the curves present the oxygen DOS weighted by the amount of, for instance, x^2-y^2 symmetry character of those oxygen states). There are two important features in this picture. In the first place the $d_{x^2-y^2}$ orbital is seen to hybridize with the top of the oxygen band, which leads to an extra stabilization of states of x^2-y^2 character with respect to other symmetry states which are bonding with respect to the Cu. In the second place the $d_{x^2-y^2}$ orbital "sees" a smaller bandwidth than the 5 eV mentioned above. These effects will give an extra stabilization to the ZR singlet. In Fig. 6 we again show the stabilization energy as a function of Δ and W. In order to speed up the calculations we did not carry out the integrations over k space [formula (3)] but we modeled the shape in Fig. 4(b) by a set of semispherical bands shown in Fig. 4(c). Figure (6) shows that the stabilization energy δ is now about 1 eV for the parameter values in Table II.

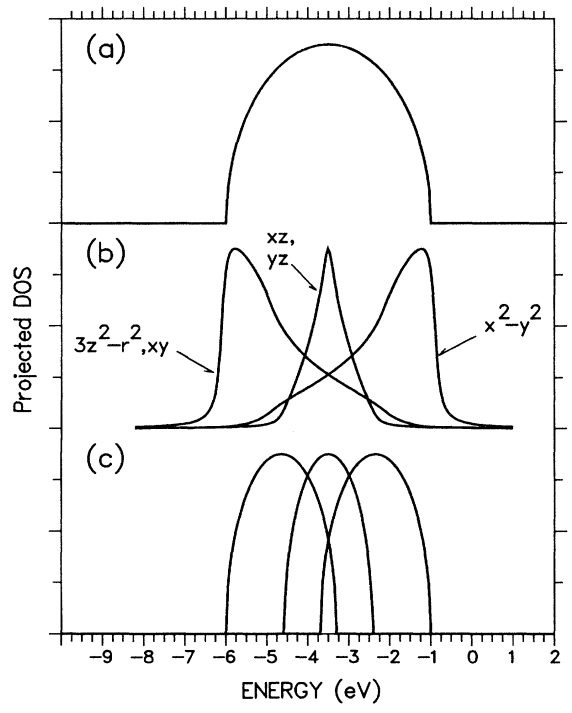

FIG. 4. Different densities of states used to model the oxygen band in the impurity case. The top curve shows a semispherical band shape. In the middle the DOS of the two-dimensional square lattice of oxygens, decomposed in d symmetry components with respect to a Cu site, is drawn. The curves are broadened with a 0.1 eV HWHM Lorentzian. The bottom curves are an approximation to the curves in (b), as explained in the text.

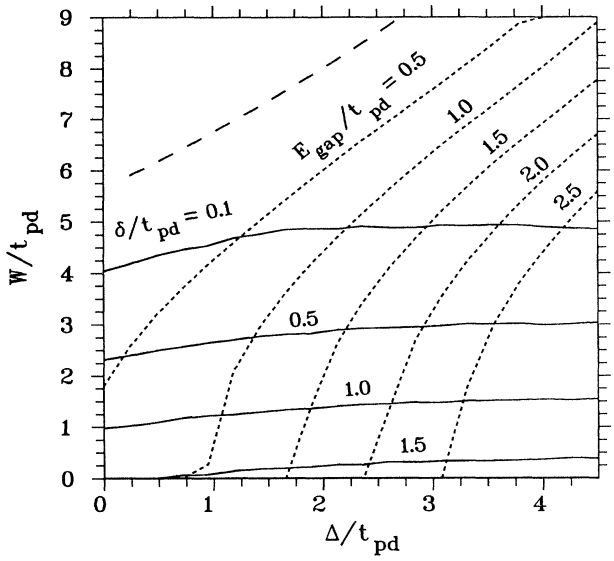

FIG. 5. Curves of constant stabilization energy (δ) of the singlet with respect to the top of the oxygen band, and curves of constant band gap ($E_{\rm gap}$), both drawn as a function of the total oxygen bandwidth (W) and the charge transfer energy (Δ). The difference between the Coulomb interaction on Cu and the charge transfer energy is kept fixed to $(A-\Delta)/t_{pd}=2.3$. The oxygen band is modeled by a semispherical density of states [see Fig. 4(a)].

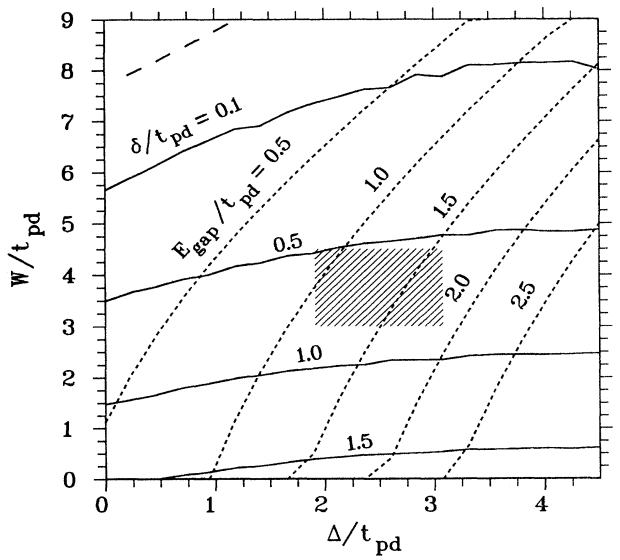

FIG. 6. Same as Fig. 5 but now with the more realistic band shape of Fig. 4(c). The hatched area indicates reasonable parameter values for the cuprates.

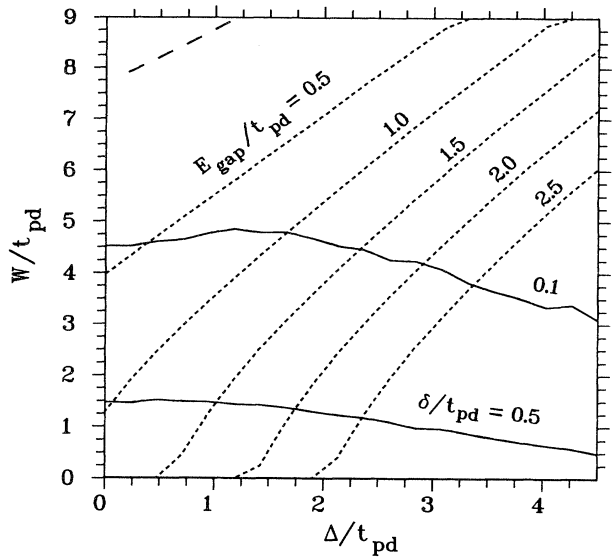

FIG. 7. Same as Fig. 6 but now for $A \rightarrow \infty$ ($U_d \rightarrow \infty$).

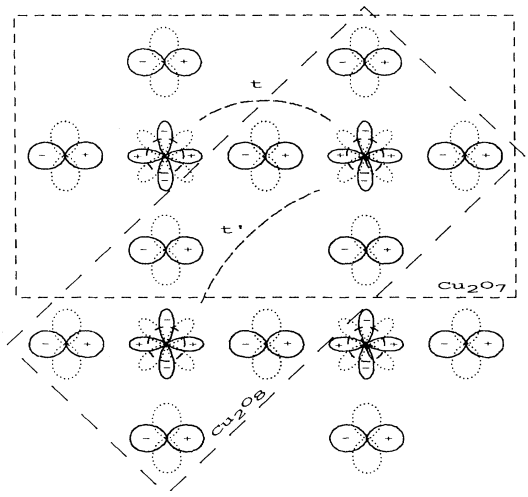

FIG. 8. The Cu_2O_7 and Cu_2O_8 clusters.

The question then is if this is sufficiently large to justify a t-J model approach.

The stability of the ZR singlet is mainly due to the very strong hybridization of the $d_{x^2-y^2}$ orbitals with the oxygens. There are two virtual hopping processes that stabilize this mainly $d^9\underline{L}$ singlet configuration, one via a $d^{10}\underline{L}^2$ state and the other via d^8. In second order the exchange energy between the ZR singlet and triplet is given by

$$J = E_s - E_T = 8t_{pd}^2 \left[\frac{1}{\Delta' + U_{pp}/4} + \frac{1}{U_{dd} - \Delta'} \right] , \quad (5)$$

where $\Delta' = \Delta + pp\sigma - pp\pi$. Thus it is very important that the value of U_d is finite and not infinite. To illustrate this we again plot the stabilization energy in Fig. 7, but now for U_d (or A) $\rightarrow \infty$. The singlet state is now again found to be very close to the oxygen band states.

IV. DISPERSION OF THE SINGLETS

Up to now we have established that the ZR singlet has a stabilization energy of about 1 eV with respect to the states of other symmetry, like the $3z^2-r^2$ symmetry states (neglecting the apex oxygen), and with respect to delocalized states on oxygen. It is now important to see if this amount is sufficient to be able to speak of a separated singlet band. For this one has to estimate the dispersional width of the ZR singlets. To do this we look at some larger clusters. Such estimates have been made before for clusters containing two Cu sites[24,26] and for clusters up to five Cu units using the three-band model.[25] The clusters we have studied are Cu_2O_7 and Cu_2O_8 shown in Fig. 8.[26] Here again all Cu $3d$ and O $2p$ orbitals are included, with the interactions on Cu given by Table I. The Coulomb and exchange multiplets on oxygen, described by F_0 and F_2, are also included. These are of importance for calculating the superexchange.

First of all we check the validity of the t-J model by mapping the lowest energy states and wave functions of the t-J model onto those of the exact three-hole problem with all orbitals included. Such a mapping has been undertaken for larger clusters, but then in a three-band model, including full local correlations in Ref. 25. This three-hole problem corresponds to doping the clusters with one extra hole. The three-hole wave functions for the t-J model as well as the corresponding triplet states are constructed from the one-hole (doubled) and two-hole singlet wave functions of a CuO_4 cluster by taking direct products

$$|R,\uparrow,S(T)\rangle = |\phi(1),\uparrow\rangle_L \otimes |\phi(2),S(T)\rangle_R , \quad (6)$$

where R (L) indicates the CuO_4 unit on the right (left) and the three-hole product states are labeled by the position of the singlet (S) or triplet (T). The eigenstates for the t-J model using this limited basis of only the L and R wave function are then easily found to be the bonding (B) and antibonding (A) sum

$$\begin{aligned} |B,\uparrow,S\rangle &= (1/\sqrt{N_B})(|R,\uparrow,S\rangle + |L,\uparrow,S\rangle) , \\ |A,\uparrow,S\rangle &= (1/\sqrt{N_A})(|R,\uparrow,S\rangle - |L,\uparrow,S\rangle) , \end{aligned} \quad (7)$$

where $N_{B(A)}$ is the normalization factor which is not 2 because $|R,\uparrow,S\rangle$ and $|L,\uparrow,S\rangle$ are not orthogonal. Note that if we would exactly follow the procedure of ZR,[38] then we would first have to orthogonalize the oxygen x^2-y^2 symmetry combination of orbitals (making Wannier orbitals) for the $Cu_2O_{7(8)}$ cluster and then create a singlet and a doublet using these. In that case the normalization factors would be 2. The energy splitting between $|B,\uparrow,S\rangle$ and $|A,\uparrow,S\rangle$ can be identified with $2t$ in the t-J model and the energy splitting between the triplet and singlet ground states for two holes in the Cu_2O_7 clus-

TABLE III. Summary of the values found for the effective singlet transfer matrix elements t and t' (hole doping), t_e and t_e' (electron doping), and the nearest- and next nearest-neighbor superexchange J and J_{NNN}. E_{gap} is the calculated band-gap energy. All energies in eV. The column "parameter" describe the deviations from the standard parameter set of Table II.

Parameter	t	t'	J	J_{NNN}	t_e	t_e'	E_{gap} Cu_2O_7	E_{gap} Cu_2O_8
...	−0.44	0.18	0.24	0.024	0.40	−0.10	2.0	2.0
$U_{pd}=1$ eV	−0.4	0.17	0.17	0.018	0.40	−0.10	2.6	2.6
$\Delta=2.5$ eV	−0.45	0.19	0.32	0.044	0.46	−0.13	1.6	1.5
$t_{pp}=0$	−0.26	0	0.08	0	0.26	0	2.6	3.0
$U_d, U_p \to \infty$	−0.27	0.17	0.05	0.005	0.40	−0.10	3.1	3.3

ter, corresponding to the insulating materials, is just the superexchange J. The Cu_2O_8 cluster calculation yields the next nearest-neighbor superexchange (J_{NNN}) and the diagonal hopping integral t', describing the next nearest-neighbor hopping of the singlet. If one neglects the oxygen bandwidth ($t_{pp}=0$), then this term is found to be quite small and is due to the finite amplitude of the oxygen Wannier states on nearest-neighbor CuO_4 units. The large value of t_{pp}, however, gives a direct hopping matrix element between singlet states on the next nearest-neighbor CuO_4 units. The values found from this mapping are given in Table III. For details we refer to Ref. 26. The value found for the singlet hopping t closely resembles the results found in Ref. 25. However, the value of t' found there is about a factor of 2 smaller than our t'. This difference is due to the nonorthogonality of singlets on neighboring Cu units.[38] This nonorthogonality leads to a competing channel for next nearest-neighbor singlet hopping via nearest-neighbor Cu units. In our opinion the value to be used for t' depends on whether or not one assumes the Zhang-Rice singlets to be orthogonal in the further treatment of the problem. If we assume them to be orthogonal, the value in Ref. 25 should be used.

The important questions are: how good is the mapping in the Cu_2O_7 cluster for both the even and the odd combinations mentioned above on the exact lowest energy states, how much Zhang-Rice triplet character is present in the two states, how much other than x^2-y^2 (i.e., $3z^2-r^2$) orbital character is present, and how large is the dispersion of the Zhang-Rice singlet? The two lowest energy states in the Cu_2O_7 cluster are the states of A_g and B_{1u} symmetry (D_{2h} point group). The amount of singlet and triplet character is determined by the overlap integrals of the wave functions $|E,\uparrow\rangle$ and $|O,\uparrow\rangle$ for singlet and triplet Zhang-Rice states with the exact eigenstates. These values are given in Table IV together with the amount of $d_{3z^2-r^2}$ in the exact eigenstates ($\langle$g.s.$|$ in Table IV denotes the exact numerical ground-state wave function and $\langle 1|$ the first excited state). The exact calculations are done for the full set of orbitals and also for the reduced set of only the $d_{x^2-y^2}$ and p_σ orbitals (three-band model). The mapping on the reduced basis is found to be extremely good (overlaps as much as 98%). Using the full basis we, however, find that for the excited state [antibonding singlet state (O) or a $\mathbf{k}$ value near the Brillouin zone boundary] the overlap is only 80%. This is due to the admixture of the $d_{3z^2-r^2}$ orbital, found to be occupied by about 10%.

The mapping of the trial wave functions onto the exact eigenstates of the cluster can be visualized by calculating their special distribution. This means evaluating the following spectrum or Green's function (in case of the bonding singlet-spin combination)

$$I(\omega)=\sum_f |\langle f|B,\uparrow,S\rangle|^2\delta(\omega-E_f)$$
$$=\frac{1}{\pi}\,\mathrm{Im}[\langle B,\uparrow,S|\hat{G}(\omega)|B,\uparrow,S\rangle]\,, \tag{8}$$

where f denotes all possible three-hole final states. The Green's function is evaluated by first evaluating the three-hole Hamilton matrices numerically and then expressing the equation above as a continued fraction.[47] In a similar manner also the spectra distribution of the singlet antibonding and the triple trial-wave functions, as well as the photoemission spectrum are evaluated. The result of this calculation is shown in Fig. 9. Figure 9(a) shows the photoemission spectrum up to 12 eV below the Fermi level for comparison. As can be seen, the singlet-doublet (S—D) bonding trial wave function (b) gives a very good representation of the lowest energy state found in the photoemission spectrum (a). The admixture of triplet character into the ground state is very small as can be seen from Fig. 9(d). The small shoulder in (b) is due to $3z^2-r^2$ admixture. According to Table IV the singlet-doublet antibonding wave function has only 80% overlap with the second energy level in Fig. 9(a). This is evident from (c) where quite some weight goes into the second subpeak. This peak has $3z^2-r^2$ character and corresponds to the $^3B_1$ state in Fig. 1. From Fig. 9(e) it can be seen that there is a small admixture of the ZR triplet in the first excited state in (a). The last two curves show that the triplet-doublet states do not represent eigenstates of the Hamiltonian, as the spectral weight is found to be distributed over many eigenstates. This is also found for the reduced basis set. The corresponding $^3A_1$ peak in

TABLE IV. Overlaps between the trial wave functions themselves and between the trial wave functions and the exact ground state $|g.s.\rangle$ and first excited state $|1\rangle$ of the Cu_2O_7 cluster. The last two numbers give the occupation of the $3z^2-r^2$ orbital on a Cu site for the exact states.

$\lvert\langle R,\uparrow,S\rvert L,\uparrow,S\rangle\rvert^2$		0.019	
$\lvert\langle R,\uparrow,S\rvert L,\uparrow,T\rangle\rvert^2$		0.012	
$\lvert\langle R,\uparrow,T\rvert L,\uparrow,T\rangle\rvert^2$		0.008	
	Full basis		Reduced basis
$\lvert\langle A,\uparrow,S\rvert 1\rangle\rvert^2$	0.80		0.98
$\lvert\langle B,\uparrow,T\rvert g.s.\rangle\rvert^2$	0.007		0.008
$\lvert\langle A,\uparrow,T\rvert 1\rangle\rvert^2$	0.011		0.014
$\langle g.s.\rvert n(d_{3z^2-r^2})\rvert g.s.\rangle$	0.013		...
$\langle 1\rvert n(d_{3z^2-r^2})\rvert 1\rangle$	0.094		...

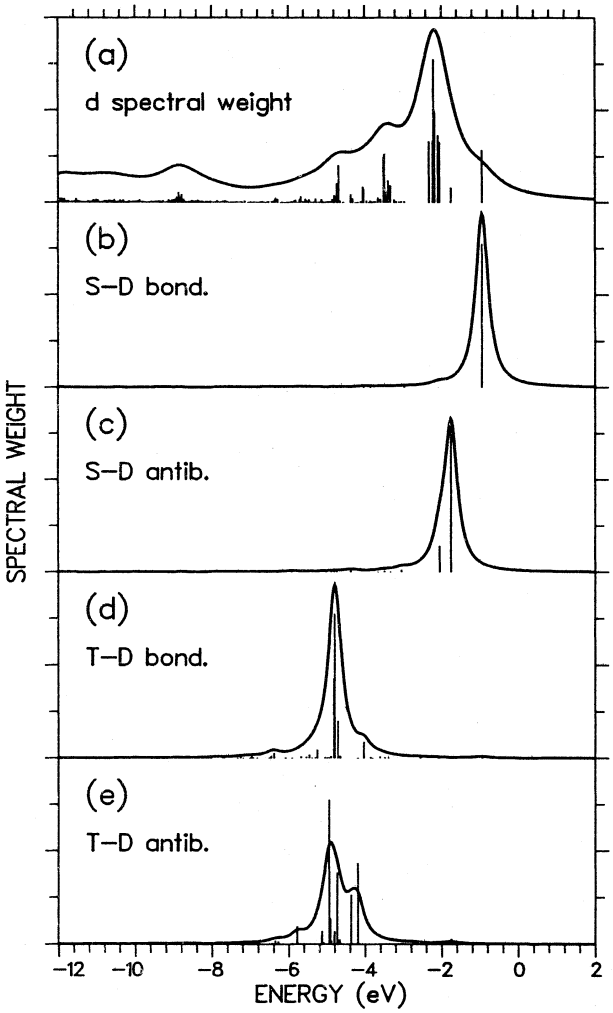

FIG. 9. The spectral distribution of the trial wave functions for the Cu_2O_7 cluster as explained in the text. The singlet-doublet bonding and antibonding spectral distributions are shown in (b) and (c), respectively. The triplet distributions are shown in (d) and (e). For comparison the d spectral weight (photoemission spectrum) is shown in (a).

Fig. 1 is found at about the same average energy. An important point is that these triplet states are about 3.5 eV higher in energy as the singlets, as already mentioned.

V. DISCUSSION

Let us first summarize what we found up to now. For the CuO_4 cluster we found a lowest energy singlet state resembling the Zhang-Rice singlet in character and symmetry. As ZR also remarked, the corresponding triplet state lies much higher in energy (about 3.5 eV). Figure 1, however, also shows that between the singlet and triplet state there is a manifold of other symmetry states, where the lowest is a triplet state involving a $3z^2-r^2$ hole. This state is separated from the singlet by about 1.5 eV.

The influence of the large oxygen bandwidth ($\simeq 5$ eV) was investigated using an impurity approach. Here we found that, due to the large Cu-O hybridization strength the singlet is still stabilized by about 1 eV with respect to the oxygen band edge. The internal structure of the oxygen band was shown to be very important in this respect.

For the three-band model the spin and symmetry of the low-energy states in the clusters containing two Cu atoms were found to correspond to what is expected in a t-J model. The dispersion of the singlet was estimated and found to be very large ($t \simeq 0.4$ eV). We argued that the t-J model, as a realistic model for the high-T_c compounds, needs an extension to a t-t'-J model, as t' is found to be large because of the oxygen dispersion. The mapping on the many-band model led to less good results, due to the admixture of $3z^2-r^2$ orbitals.

Returning to the amount of $3z^2-r^2$ character. Note that there are two effects that we did not discuss here. In the first place we neglected the crystal-field splittings between the different Cu d orbitals and all ε_α energies were taken to be the same. The strong stabilization of the x^2-y^2 orbital is in our calculation due entirely to the large value of t_{pd}. The influence of orbitals other than Cu $3d$ and O $2p$ tends to favor the x^2-y^2 orbital energetically even more,[41] placing the $3z^2-r^2$ orbital about 0.5 eV higher in energy. In the second place we chose to focus on the CuO_2 planes, thus neglecting the apical oxy-

gens, in order to keep the discussion general. These apex oxygens have the opposite effect of stabilizing the $3z^2-r^2$ orbitals.[21,23] In the limit of a cubic surrounding of the Cu, the point symmetry group of a CuO_6 cluster is O_h and the x^2-y^2 and $3z^2-r^2$ orbitals are degenerate (e_g orbitals). These effects will depend strongly on the position and number of apical oxygens, and thus will be dependent on the materials. Another important point is that the x^2-y^2 and $3z^2-r^2$ bands are mixed in the real solid (which was symmetry forbidden for the small CuO_4 cluster). This mixing will be strongest for $\mathbf{k}$ values close to $(\pi,0)$. For $e_d(x^2-y^2)=e_d(3z^2-r^2)$ and along the line $\mathbf{k}=(0,0)$ to $(\pi,0)$, we have

$$\frac{n(d_{x^2-y^2})}{n(d_{3z^2-r^2})}=\frac{t_{pd}^2(x^2-y^2)}{t_{pd}^2(3z^2-r^2)}\simeq 3 . \tag{9}$$

This would mean the $3z^2-r^2$ is admixed by about 25% in the one-particle Bloch states for $\mathbf{k}$ values close to $(\pi,0)$. Grant and McMahan[48] have recently shown, using a Hartree-Fock approach with limited configuration interaction, that these $3z^2-r^2$ orbitals could be of quite some importance for states close to the Fermi level.

Emery and Reiter (ER, Ref. 39, for related papers see Refs. 49–51) have argued that especially the spin properties of the single-band model are not equivalent to those of the three-band model. Their point is illustrated with an exact solution of one oxygen hole propagating in a ferromagnetic lattice of Cu spins, in the limit of U_d, $\Delta\rightarrow\infty$ and $(U_d-\Delta)/t_{pd}$ large. The solution consists of Fourier-transformed local singlet states made out of a Cu spin and a hole on the four oxygen sites surrounding the Cu (states $P_{i,\sigma}$). Therefore singlet states on neighboring Cu units are not orthogonal to each other. ER show that this solution consisting of nonorthogonal singlets can be written approximately as a sum of (orthogonal) Fourier-transformed ZR singlet and ZR triplet states and that this mixing between singlets and triplets is as large as 50% for $\mathbf{k}=(\pi,\pi)$. This mixing of singlets and triplets will then give rise to a finite spin (and nonzero spin-spin correlation functions) on the oxygen, as opposed to the zero-spin contribution from the singlet states in the one-band model.

In the $Cu_2O_{7,8}$ clusters we compared the exact states with nonorthogonal singlet and triplet trial wave functions, a construction very similar to the exact eigenstates found by Emery and Reiter. These states were found to be a very accurate description of the low-energy states and the admixture of (nonorthogonal) triplet states was found to be very small (Table IV and Fig. 9). These results suggest that after inclusion of correlations on the oxygen, the oxygen-oxygen hopping t_{pp} and the effects of the strong hybridization t_{pd} (leading to a significant redistribution of charge from the Cu to the oxygen), the exact eigenstates are still fairly well described by a wave function consisting of nonorthogonal singlet states in a spin lattice, and thus very similar to the wave function found by ER. This demonstrates the large stabilization energy of the singlet states for a large part of parameter space. Note that the "spin" state is now a strongly hybridized wave function

$$|\phi(1),\uparrow\rangle=\alpha|d_{x^2-y^2},\uparrow\rangle+\beta|\tfrac{1}{2}(p_1+p_2+p_3+p_4)\uparrow\rangle$$

and the singlet state also involves d^8 and $d^{10}\underline{L}^2$ configurations.

To study the amount of ZR triplet character (orthogonal oxygen states) in the exact eigenstates, we also investigated the Emery-Reiter limit U_d, $\Delta\rightarrow\infty$ and $(U_d-\Delta)/t_{pd}$ large and $t_{pp}=0$. In this limit the hybridization is negligible and one can construct orthogonal wave functions similar to the Zhang-Rice construction by starting with orthogonal oxygen states ($\phi_{i,\sigma}, i=1$ or 2) localized on the left (1) or right (2) Cu unit and then creating singlet-doublet trial wave functions with these. The overlap of these states with the exact eigenstates is again found to be very large (>98% ZR singlet bonding/antibonding character for the ground/first excited state). The admixture of ZR triplets in the exact low-energy states is very small in both cases ($\simeq 1\%$). The same good correspondence holds for the spin S_z on the central oxygen site in the cluster. For the nonorthogonal trial wave functions one finds $S_z=-1/18$ for the bonding state and $S_z=1/14$ for the antibonding combination. For the Zhang-Rice construction this is $S_z=-1/20$ and $1/20$, respectively. This shows that also the spin is not very different for both states in the cluster. In general for the Cu_2O_7 cluster both the Zhang-Rice and the nonorthogonal trial wave functions give an excellent description of the low-energy states, in contrast with the results of ER for large $\mathbf{k}$ values for the infinite lattice. The reason for this is that in the Cu_2O_7 cluster there is only one neighboring Cu unit instead of four in the CuO_2 plane. This means that singlets on neighboring sites feel the orthogonality constraint only in a largely reduced manner. Even without the central oxygen site one can still construct a singlet state with a large stabilization energy using only other three O atoms around the Cu. To our opinion these small clusters are therefore not suited to estimate the amount of ZR triplet admixture.

As is shown above, the Zhang-Rice construction also leads to a finite spin value on the oxygen site. A more instructive number is the spin divided by the occupation. This is $-1/6$ for the bonding function and $1/2$ (or maximal!) for the antibonding state for the central oxygen. (Note that the spin of the orthogonal oxygen states $\phi_{i,\sigma}$ is zero.) Thus ZR singlets are not singlets in the sense that all spin values and spin-spin correlation functions are strictly zero! The reason for this is the nonorthogonality of the $P_{i,\sigma}$ states, leading to singlets which are not separated in space. Therefore the spin operator S_z will couple singlet states on nearest-neighbor Cu units. This also holds for the infinite plane. Using Eq. (8) of Ref. 39 which describes a normalized Fourier-transformed Zhang-Rice singlet state $|\phi_{\mathbf{k}}\rangle$, we find

$$\langle\phi_{\mathbf{k}}^-|\hat{S}_z(p_x)|\phi_{\mathbf{k}}^-\rangle=\frac{1}{8N}\frac{\cos(k_x)-\cos(k_y)}{2+\cos(k_x)+\cos(k_y)} ,$$

$$\langle\phi_{\mathbf{k}}^-|\hat{S}_z(p_y)|\phi_{\mathbf{k}}^-\rangle=-\langle\phi_{\mathbf{k}}^-|\hat{S}_z(p_x)|\phi_{\mathbf{k}}^-\rangle .$$

Here p_x is the O $2p$ orbital on one of the oxygens in the

three-band model pointing towards the Cu and p_y the orbital on the second oxygen site. Thus apart from the admixture of triplets the ZR singlets themselves may lead to a spin on the oxygens. The actual charge and spin distribution behind the Zhang-Rice construction is far more complicated than that suggested by the t-J model.

In conclusion, we have shown that "singlets" seem to be the dominating objects for the low-energy physics, but that one cannot speak of a clearly separated singlet band. The high-energy states in the one-band model will overlap with states with symmetries other than x^2-y^2 and the admixture of $3z^2-r^2$ could be important. The states of a three-band model (triplet excitations) that are not described by the t-J or t-t'-J model are found to be very high in energy and a manifold of other symmetry states are found in between the singlet and triplet states. This is why we would say that if single-band Hubbard is not appropriate then neither is a three-band model.

[1]Z.-X. Shen *et al.*, Phys. Rev. B **36**, 8414 (1987).

[2]A. Fujimori, E. Takayama-Muromachi, Y. Uchida, and B. Okai, Phys. Rev. B **35**, 8814 (1987).

[3]O. Gunnarsson *et al.*, Phys. Rev. B **41**, 4811 (1990).

[4]M. R. Thuler, R. L. Benbow, and Z. Hurych, Phys. Rev. B **26**, 669 (1982).

[5]J. Ghijsen *et al.*, Phys. Rev. B **38**, 11 322 (1988).

[6]N. Nücker, J. Fink, J. C. Fuggle, P. J. Durham, and W. M. Timmerman, Phys. Rev. B **37**, 5158 (1988).

[7]J. A. Yarmoff, D. R. Clarke, W. Drube, U. O. Karlsson, A. Taleb-Ibrahim, and F. J. Himpsel, Phys. Rev. B **36**, 3967 (1987).

[8]P. Kuiper *et al.*, Phys. Rev. B **38**, 6483 (1988).

[9]J. Zaanen, G. A. Sawatzky, and J. W. Allen, Phys. Rev. Lett. **55**, 418 (1985).

[10]C. A. Balseiro, M. Avignon, A. G. Rojo, and B. Alascio, Phys. Rev. Lett. **62**, 2624 (1989).

[11]B. Jin, M. Avignon, and K. H. Bennemann, Europhys. Lett. **13**, 447 (1990).

[12]R. J. Birgeneau and G. Shirane, in *Physical Properties of High Temperature Superconductors I,* edited by Donald M. Ginsberg (World Scientific, Singapore, 1989), p. 152.

[13]P. B. Allen, Z. Fisk, and A. Migliori, in *Physical Properties of High Temperature Superconductors I* (Ref. 12), p. 213.

[14]R. E. Walstedt and W. W. Warren, Jr., in *Mechanisms of High Temperature Superconductivity,* edited by H. Kamimura and A. Oshiyama, Springer Series in Material Science, Vol. II (Springer-Verlag, Berlin, Heidelberg, 1989), p. 137.

[15]M. Takigawa, P. C. Hammel, R. H. Heffner, and Z. Fisk, Phys. Rev. B **39**, 7371 (1989).

[16]J. L. Budnick *et al.*, Europhys. Lett. **5**, 651 (1988).

[17]D. R. Harshman *et al.*, Phys. Rev. B **852**, (1988).

[18]Y. J. Uemura *et al.*, Phys. Rev. Lett. **59**, 1045 (1987).

[19]P. E. Sulewski, P. A. Fleury, K. B. Lyons, S.-W. Cheong, and Z. Fisk, Phys. Rev. B **41**, 225 (1990).

[20]M. Takigawa, P. C. Hammel, R. H. Heffner, Z. Fisk, K. C. Ott, and J. D. Thompson, Physica C **162-164**, 853 (1989); M. Takigawa, in *High Temperature Superconductivity,* Proceedings of the Los Alamos Symposium 1989, Los Alamos, New Mexico, edited by K. Bedell, D. Coffey, D. E. Meltzer, D. Pines, and J. R. Schrieffer (Addison-Wesley, Reading, 1990), p. 236.

[21]A. Fujimori, Phys. Rev. B **39**, 793 (1989).

[22]F. Mila, Phys. Rev. B **38**, 11 358 (1988).

[23]H. Eskes, L. H. Tjeng, and G. A. Sawatzky, Phys. Rev. B **41**, 288 (1990).

[24]S. Maekawa, J. Inoue, and T. Tohyama, in *Strong Correlation and Superconductivity,* edited by H. Fukuyama, S. Maekawa, and A. P. Malozemoff, Springer Series in Solid-State Science, Vol. 89 (Springer, New York, 1989), p. 66; Y. Ohta, T. Tohyama, and S. Maekawa, Phys. Rev. B **43**, 2968 (1991).

[25]M. S. Hybertsen, E. B. Stechel, M. Schluter, and D. R. Jennison, Phys. Rev. B **41**, 11 068 (1990).

[26]H. Eskes, G. A. Sawatzky, and L. F. Feiner, Physica C **160**, 424 (1989).

[27]H. Eskes and G. A. Sawatzky, Phys. Rev. Lett. **61**, 1415 (1988).

[28]A. K. McMahan, R. M. Martin, and S. Satpathy, Phys. Rev. B **38**, 6650 (1988).

[29]A. Bianconi *et al.*, Physica C **153-155**, 1760 (1988); A. Bianconi *et al.*, in *High T_c Superconductors: Electronic Structure,* Proceedings of the International Symposium, Rome, 5–7 October 1988, edited by A. Bianconi and A. Marcelli (Pergamon, New York, 1989), p. 281.

[30]B. Batlogg, in *High Temperature Superconductivity* (Ref. 20), p. 37.

[31]P. W. Anderson, Phys. Rev. **124**, 41 (1961).

[32]W. Weber, Z. Phys. B **70**, 323 (1988).

[33]A. M. Oleś and J. Zaanen, in *Recent Progress in Many Body Theories,* edited by I. Avishai (Plenum, New York, 1990), Vol. 2.

[34]H. Kamimura, in Proceedings of the Conference Towards the Theoretical Understanding of High T_c Superconductors, Trieste, July 1988, edited by S. Lundqvist, E. Tosatti, M. P. Tosi, and Yu Lu [Int. J. Mod. Phys. **1**, 699 (1988)].

[35]V. J. Emery, Phys. Rev. Lett. **58**, 2794 (1987).

[36]C. M. Varma, S. Schmitt-Rink, and E. Abrahams, in *Novel Superconductivity,* Proceedings of the International Conference on New Mechanisms of Superconductivity, Berkeley, 1987, edited by V. Kresin and S. Wolf (Plenum, New York, 1987), p. 355.

[37]P. W. Anderson, Science **235**, 1196 (1987).

[38]F. C. Zhang and T. M. Rice, Phys. Rev. B **37**, 3759 (1988).

[39]V. J. Emery and G. Reiter, Phys. Rev. B **38**, 11 938 (1988); **41**, 7247 (1990).

[40]M. S. Hybertsen, M. Schlüter, and N. E. Christensen, Phys. Rev. B **39**, 9028 (1989).

[41]A. K. McMahan, J. F. Annett, and R. M. Martin, Phys. Rev. B **42**, 6268 (1990).

[42]J. Kanamori, Prog. Theor. Phys. **30**, 275 (1963).

[43]G. A. Sawatzky, Phys. Rev. Lett. **39**, 504 (1977).

[44]J. Zaanen, Ph.D. thesis, University of Groningen, 1986.

[45]F. D. M. Haldane and P. W. Anderson, Phys. Rev. B **13**, 2553 (1976).

[46]J. F. Annett and R. M. Martin, Phys. Rev. B **42**, 3929 (1990).

[47]*Memory Function Approaches to Stochastic Problems in Condensed Matter,* edited by M. W. Evans, P. Grigolini, and G. Pastori Parravicini, Wiley series on Advances in Chemical Physics, Vol. 62 (Wiley, New York, 1985).

[48]J. B. Grant and A. K. McMahan, Phys. Rev. Lett. **66**, 488 (1991).

[49]F. C. Zhang, Phys. Rev. B **39**, 7375 (1989).

[50]R. J. Gooding and V. Elser, Phys. Rev. B **41**, 2557 (1990); F. C. Zhang and T. M. Rice, *ibid.* **41**, 2560 (1990).

[51]F. C. Zhang and T. M. Rice, Phys. Rev. B **41**, 7243 (1990).